NASA TECHNICAL MEMORANDUM

NASA TM X-1333

NASA TM X-1333

EVALUATION OF A THIN-FILM, HEAT-FLUX PROBE FOR MEASURING GAS VELOCITIES IN AN UNSTABLE ROCKET COMBUSTOR

by Frederick P. Povinelli and Robert D. Ingebo

Lewis Research Center
Cleveland, Ohio

NATIONAL AERONAUTICS AND SPACE ADMINISTRATION • WASHINGTON, D. C. • FEBRUARY 1967

NASA TM X-1333

EVALUATION OF A THIN-FILM, HEAT-FLUX PROBE FOR MEASURING GAS VELOCITIES IN AN UNSTABLE ROCKET COMBUSTOR

By Frederick P. Povinelli and Robert D. Ingebo

Lewis Research Center
Cleveland, Ohio

NATIONAL AERONAUTICS AND SPACE ADMINISTRATION

For sale by the Clearinghouse for Federal Scientific and Technical Information
Springfield, Virginia 22151 – Price $1.00

EVALUATION OF A THIN-FILM, HEAT-FLUX PROBE FOR MEASURING GAS VELOCITIES IN AN UNSTABLE ROCKET COMBUSTOR

by Frederick P. Povinelli and Robert D. Ingebo

Lewis Research Center

SUMMARY

The use of a heat-flux probe to measure gas velocities in an unstable rocket combustor was evaluated. The combustor burned ethanol and liquid oxygen at an oxidant- to fuel-mass ratio of 0.9 at an average chamber pressure of 178±2 pounds per square inch absolute. Measurements were made of heat transfer from combustion gases to a water-cooled, thin-film sensor. Gas velocities calculated from the heat-transfer data were generally more than a factor of two larger than velocities measured from streak photographs. A correction applied to the heat-flux signal resulted in better agreement. Maximum streak velocities and maximum velocities calculated from pressure measurements agreed to within 3 percent.

INTRODUCTION

Research and development programs have brought forth a wealth of information on rocket-engine systems operating in unstable modes of oscillation. Theories of propellant behavior in oscillating fields have been expounded analytically and tested experimentally, as in references 1 and 2, respectively. Application of the results of such studies requires a knowledge of the local value and behavior of the combustion gas velocity.

The methods available for measuring combustion gas velocities have been limited mainly to streak photography (ref. 3). Since the combustion gases must be luminous and have large density and/or temperature gradients for sharp images, streak photography is not always practical. Probably the most serious drawback of this technique, however, is that highly localized velocities cannot be obtained. Other methods such as Mach num-

ber determination from Pitot-tube readings or hot-wire anemometry require that the probing instrument be able to withstand the combustion environment and possess adequate frequency response. This investigation was undertaken to obtain reliable local gas velocity measurements within a combustor operating unstably.

Velocity measurements were obtained by employing a commercially available, water-cooled, thin-film, heat-flux probe (refs. 4 and 5) in a cylindrical combustor. The combustor burned ethanol and liquid oxygen at an average chamber pressure of 178±2 pounds per square inch absolute. Peak-to-peak longitudinal pressure oscillations of 15 percent were sustained at 1190±5 cps with a siren mounted directly downstream of the exhaust nozzle. Streak photographs provided an alternative method of obtaining gas velocities. Gas velocities were also calculated from chamber-pressure measurements. The velocities obtained by these techniques were compared.

APPARATUS

Heat-Flux System

The commercially available heat-flux measuring system consisted of three main components: a sensing element, a sensor-holding probe, and electronic circuitry. Each of these components is described separately.

Sensing element. - The heat-flux sensing element (fig. 1) consisted of a plated, looped, cylindrical tube. The tube material was 96 percent silica, its outside diameter was 0.006 inch, and its inside diameter was 0.004 inch. The distance between the two

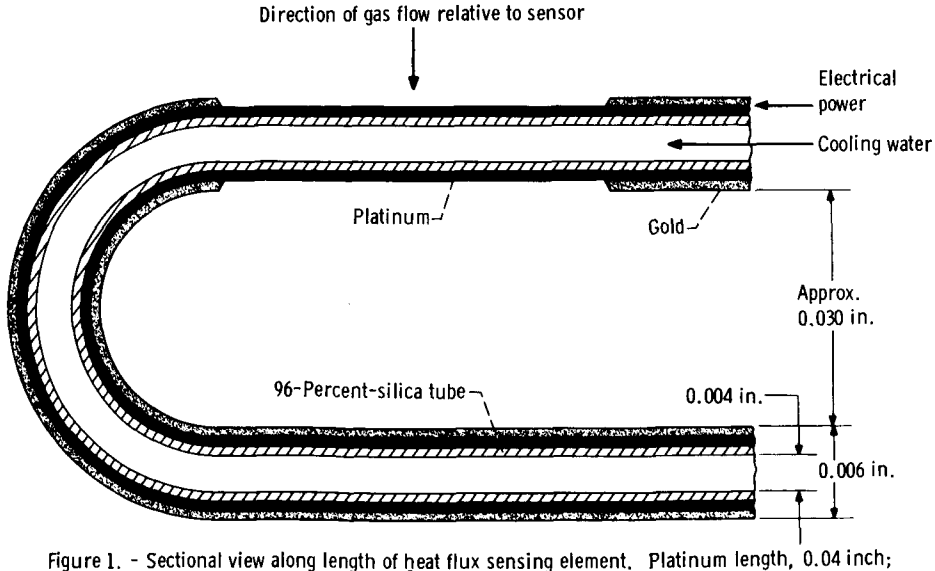

Figure 1. - Sectional view along length of heat flux sensing element. Platinum length, 0.04 inch; platinum thickness, approximately 600 Å.

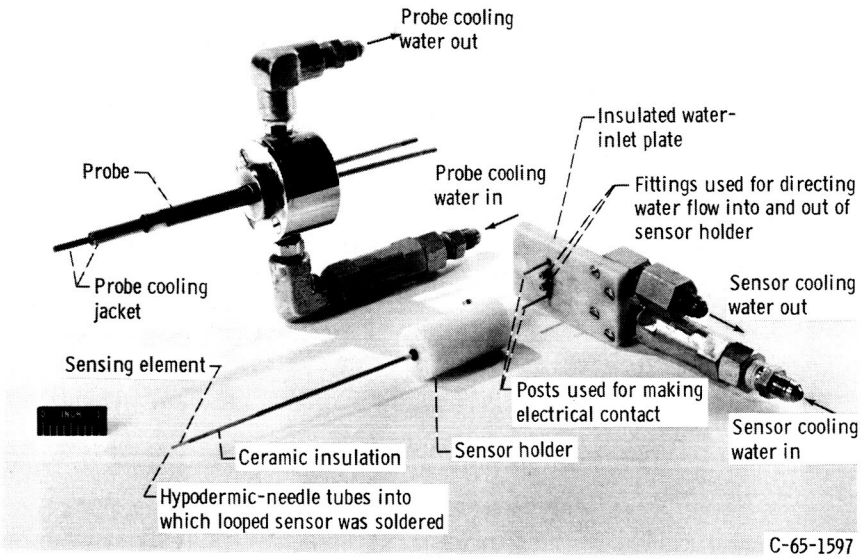

(a) Unassembled.

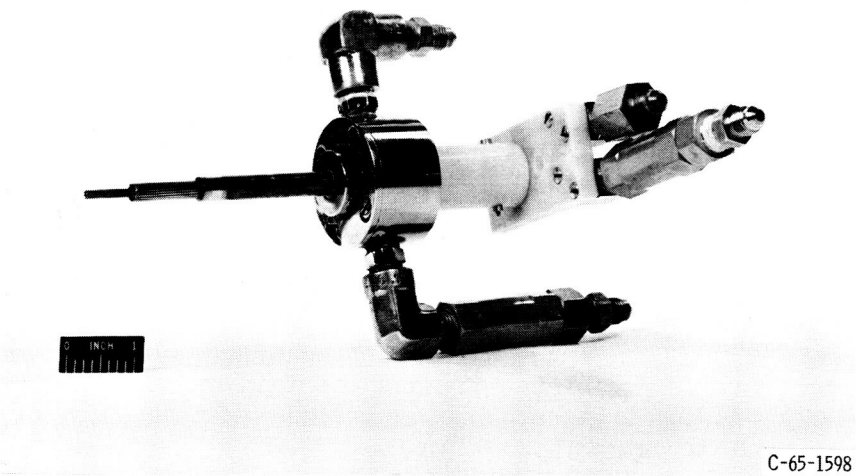

(b) Assembled.

Figure 2. - Probe apparatus.

legs of the loop was approximately 5 tube outside diameters. A platinum film approximately 600 Å (2.4×10^{-6} in.) thick was chemically deposited over the entire length of the tube. A layer of gold was similarly deposited over the platinum in such a way as to expose a 0.04-inch length of sensitive platinum film. The passage through the tube permitted water cooling.

Sensor holder and probe. - The sensor was soldered into stainless-steel hypodermic-needle tubing mounted in an insulated sensor holder (fig. 2(a), p. 3). The sensor holder was so inserted into the probe that the platinum element protruded approximately 0.04 inch from the end of the water-cooled jacket (fig. 2(b)). The probe jacket consisted of a series of water-cooled tubes, which provided protection to the sensor mounting. Thus assembled, the probe was attached to the rocket chamber. Distilled water under a pressure of 1100 pounds per square inch gage was directed through the sensor, and tap water under a pressure of 250 pounds per square inch gage was directed through the probe.

Electronic circuitry. - The electronic circuitry used was similar to that used in constant-temperature hot-wire anemometry. The sensor was connected as one leg of a Wheatstone bridge (fig. 3). The platinum surface was maintained at constant resistance and hence constant temperature. This surface temperature was predetermined by setting the value of the variable resistance R_1. Any change in platinum temperature due to an environment change was detected as a bridge off balance. This error signal was amplified and fed to the power amplifier, which changed the current supplied to the sensor enough to restore the bridge balance. The frequency response of the overall system depends on the environment and on the sensor operating level and dimensions. In reference 4, the response of the electronic circuitry in high-temperature gases is stated to be nearly flat to 10 000 cps. The electrical power to the sensor was made available as output by feeding the bridge voltage through a squaring circuit (power computer).

Method of operation. - In a rocket combustion environment, the platinum sensor measures the rate of heat transfer from the environment to the sensor. The cooling-

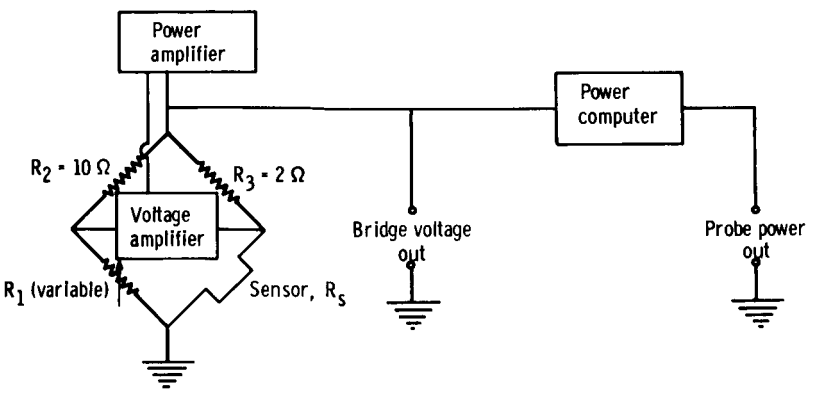

Figure 3. - Bridge and amplifier circuitry.

water flow rate through the sensor determines the amount of heat which can be dissipated in the sensor either electrically or from the external environment. The heat balance written for the platinum sensing surface is

$$3.413\ I^2R_s = P = hA(T_s - T_e) + UA(T_s - T_w) \tag{1}$$

(All symbols are defined in the appendix.) Since the platinum temperature was held constant by the electronic circuitry, and the water flow rate and the temperature were also held constant, the last term in equation (1) is a constant C. In still air, the heat generated electrically in the platinum film is dissipated nearly entirely in the water. Thus, in a combustion gas environment, the change in power to the sensor is the change in heat transfer between the environment and the sensor:

$$C - P = hA(T_e - T_s) = Q \tag{2}$$

Combustion Chamber

The rocket combustor in which velocity measurements were made is described in detail in reference 2. The modified engine section used to house the heat-flux probe is shown in figure 4. The probe was mounted 14.5 inches downstream of the injector and was so inserted into the chamber that the platinum sensing element was located on the combustor axis.

Large pressure gradients during the startup and shutdown sequences of the engine and liquid drops impinging on the sensor during startup necessitated protecting the sensor with a shield. The shield consisted of a 5/8-inch-outside-diameter stainless-steel tube drilled with a series of thirty-eight 1/16-inch-diameter holes on the bottom side. This tube allowed the sensor to be exposed to upward velocity in the chamber while it was shielded. The shielding tube was attached to the shaft of a pneumatic piston and mounted directly across the chamber from the heat-flux probe. The shielding tube was retracted flush with the chamber wall during the main data-taking portion of the combustion run.

A water-cooled, wire-strain-gage pressure transducer was flush-mounted 2.5 inches downstream from the heat-flux-probe location. Other modified engine sections, one containing a window port and the other another pressure transducer, were also used in place of the heat-flux-probe engine section. These sections allowed streak photographs and pressure measurements to be made at the heat-flux-probe station. The window section housed a 2-inch-diameter heat-resistant glass window. A vertical slit, 0.02 inch wide, was positioned on the window.

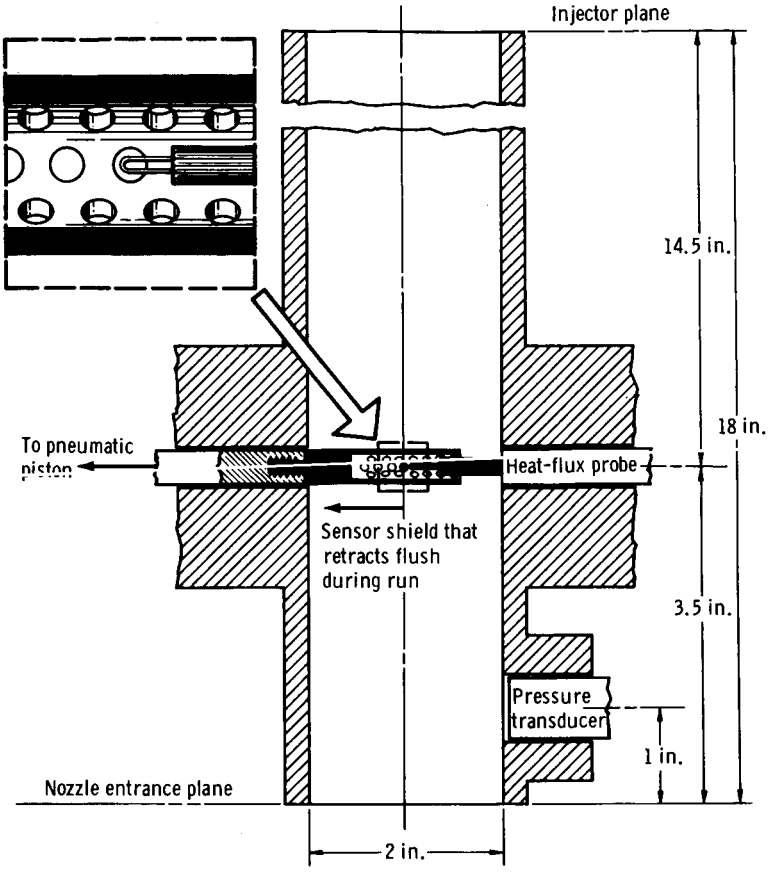

Figure 4. - Combustion chamber and instrumentation location.

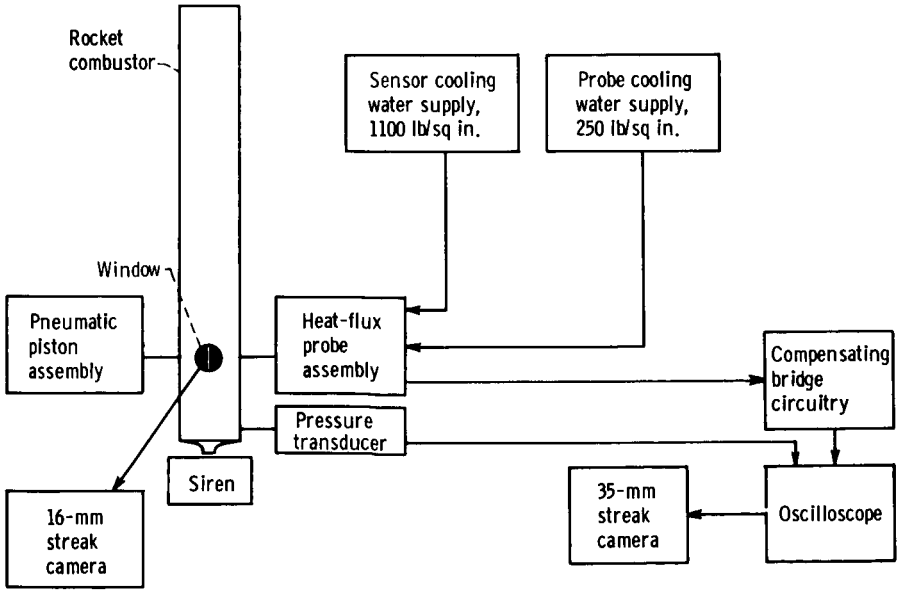

Figure 5. - Velocity measuring techniques.

Velocity-Measuring Apparatus

A schematic diagram of the velocity-measuring apparatus is shown in figure 5. The outputs from the heat-flux probe and from the pressure transducer were displayed simultaneously on a dual-beam oscilloscope. Signal changes were so displayed that beam deflections occurred in the vertical direction. A 35-millimeter high-speed streak camera positioned horizontally was used to provide a sweep of the scope deflections on film. Streak photographs of the combustion gases were taken through the window slit with a horizontally positioned 16-millimeter high-speed streak camera.

PROCEDURE AND DATA REDUCTION

First attempts at obtaining heat-flux data were hindered either by physical breakage of the sensing tube or by deterioration of the platinum and gold films. Physical breakage was nearly eliminated by use of the shielding tube. Deterioration, flaking, and peeling

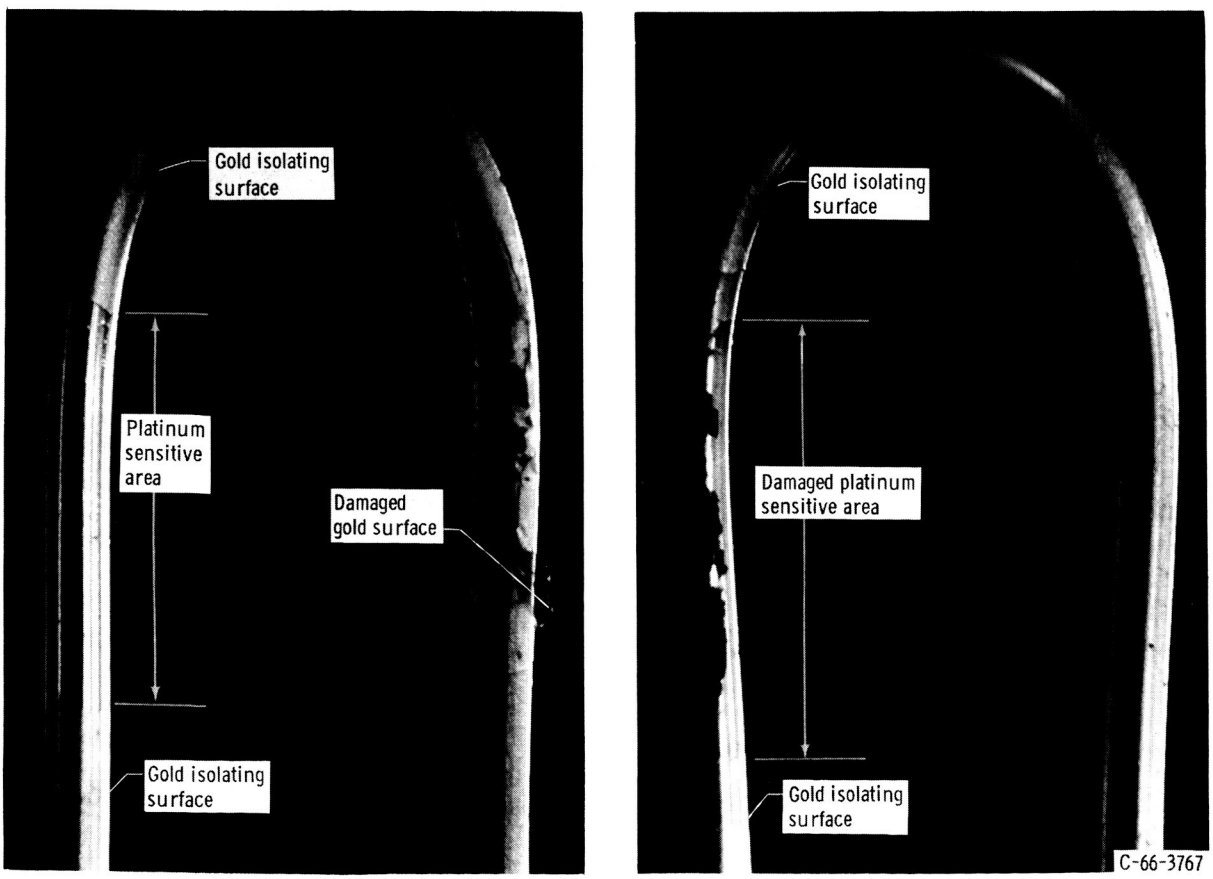

(a) Damage to gold surface.

(b) Damage to platinum surface.

Figure 6. - Sensors with damage incurred during combustion runs shown.

of the films remained a problem for the entire program. A sensor on which the gold layer cracked and began to peel is shown in an enlarged photograph (fig. 6(a)). Figure 6(b) shows a sensor on which part of the platinum layer disappeared, as shown by the darkened areas. Data were evaluated only for sensors which remained intact for the entire run.

For the heat-flux data reported herein, the initial electrical power input to the sensing element was 20.0 watts. This input represents a heat dissipation of 25.4 Btu per square inch - second in the sensor. After the sensor had been subjected to the combustion environment, the sensor power input dipped to 18.8 watts; this change in the power input was permanent.

This problem was also encountered in reference 6, where a similar sensor was positioned in the flame of an oxyacetylene torch. This change in power was due to a change in sensor resistance, probably caused by loss of some of the platinum film. Reference 6 indicates that any resistance changes occur in discrete steps and not continuously. The heat-flux data were taken near the end of the 1.5-second combustion run, and thus it could be assumed that the resistance changes had already taken place. Thus, 18.8 watts was used as the constant C in equation (2).

The pressure and streak-velocity data, as well as the heat-flux data, were analyzed near the end of each run, where the 15-percent peak-to-peak pressure oscillations were well established. These data were generally not reproducible from cycle to cycle. Thus, representative cycles for the pressure, streak velocity, and heat-flux data were obtained by averaging five or more cycles.

Typical heat-flux sensor output taken from the 35-millimeter film for a time period near the end of the combustion run is shown in figure 7(a). Heat transfer to the sensor from the environment is plotted against time. The regions of high heat transfer occur every 0.84 millisecond, and the shape and the amplitude are fairly reproducible. The regions of lower heat flux are generally composed of three oscillations with irregular shape and variable amplitude.

The output trace of the heat-flux probe averaged over five cycles is shown in figure 7(b). The average scatter about the average curve is approximately ±15 percent. The abscissa is plotted as dimensionless time t/t_{cy}, which is the ratio of the time at any point in the cycle to the time for one cycle or the period.

One of the parameters which affects the heat transfer to the sensor is the velocity of gas flow over its surface. The sensor, however, is unable to distinguish the direction of the flow. The siren, which produced the pressure oscillations in the chamber for these tests, also caused the gas flow to reverse directions periodically and to flow momentarily toward the injector. It was thus necessary to determine which portion of the cycle of the average heat-transfer curve was affected by the reverse flow. This determination was accomplished by analyzing the heat-flux output when the sensor was covered by the per-

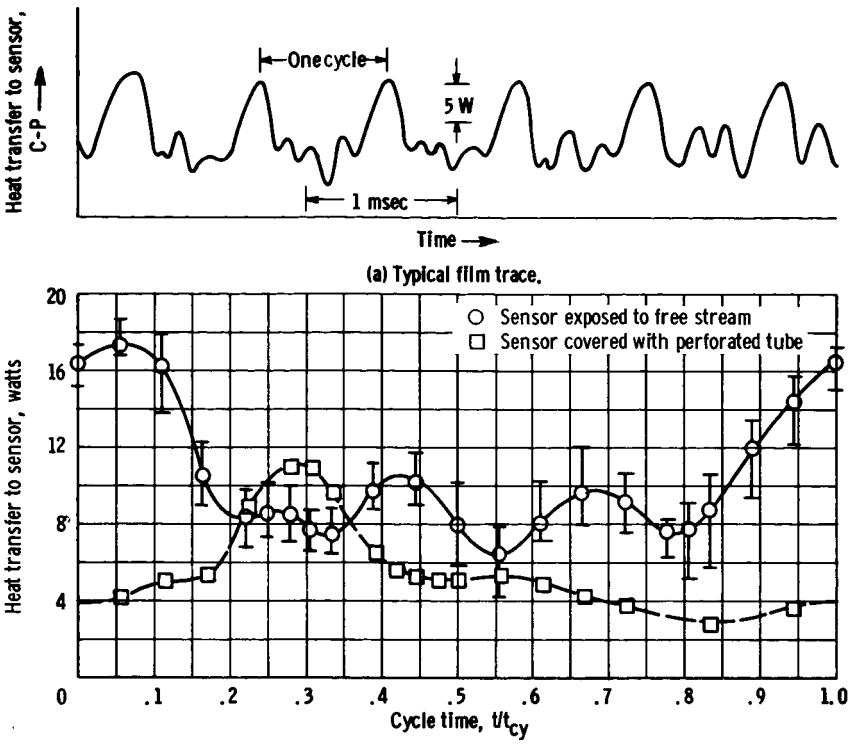

Figure 7. - Typical heat-flux sensor output and average heat flux for one cycle of oscillation.

forated tube. A portion of this output, averaged in the same way as the uncovered sensor data, is also shown in figure 7(b). When shielded, the sensor was unable to sense downstream flow velocity but could respond to upstream flow velocity. The large increase in heat transfer shown on the curve for the covered sensor indicates an upward flow velocity. This increased heat transfer corresponds to the small hump in the uncovered-sensor data for $0.22 \leq t/t_{cy} \leq 0.32$. Thus, when velocity is calculated from the heat-flux-probe output, this region must be regarded as a region of reverse flow. There also appears to be a slight increase in heat transfer at a value of t/t_{cy} of 0.55 for the covered sensor. The reverse flow causing this increase does not appear large enough to affect the uncovered-sensor trace.

In order to evaluate gas-velocity measurements calculated from heat-flux measurements, it is advantageous to determine velocities by other techniques for comparison. As mentioned previously, streak photography is the most common technique used, and although it has some limitations, it does provide a velocity measurement. A typical film strip of the streak photographs obtained in this study is shown in figure 8(a). The film speed was maintained at 320 feet per second, and the lens system produced a magnification of 0.5. Gas velocities were determined by measuring the angle between the

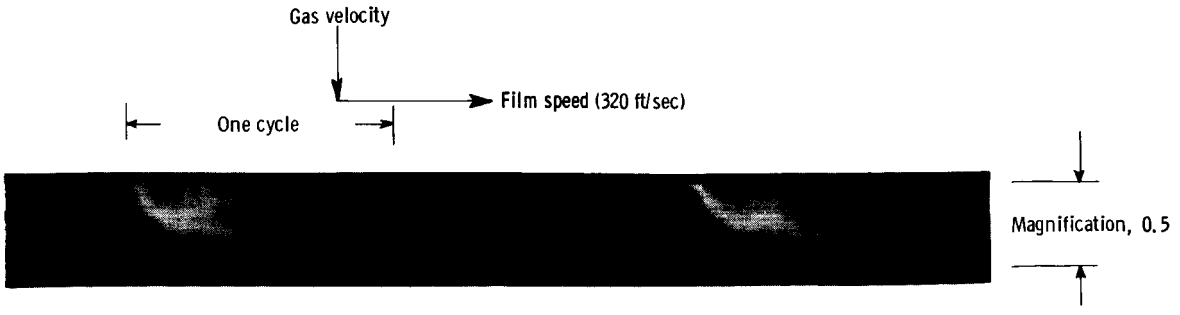

(a) Typical streak photograph of gas in rocket combustion chamber.

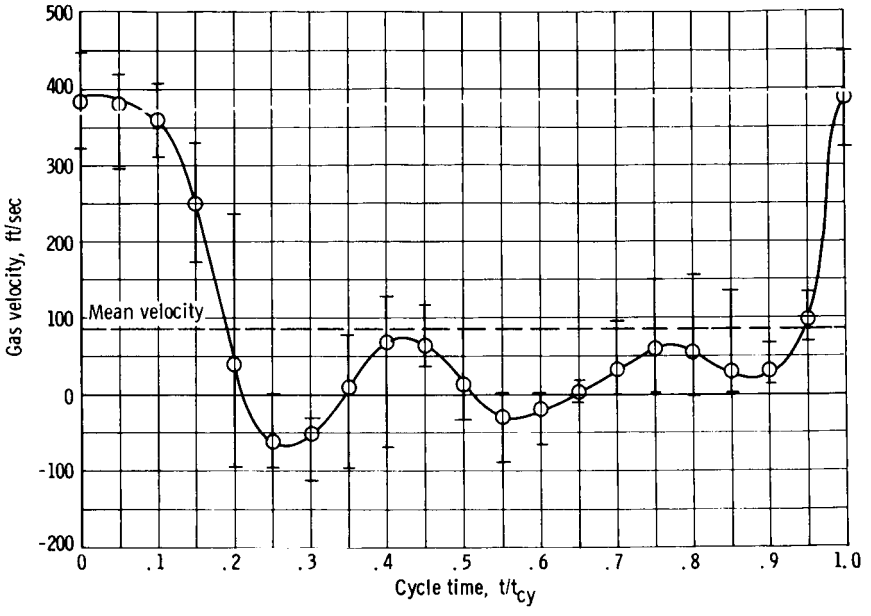

(b) Gas velocity for one cycle (averaged over six cycles).

Figure 8. - Typical streak photograph and average gas velocity for one cycle.

vertical axis and the line of demarcation of luminous and nonluminous gases and by using

$$v_g = \frac{v_f}{m \tan \theta} \tag{3}$$

The time between bursts of high-velocity luminous gas was 0.84 millisecond, the same time measured for one cycle from the heat-flux data.

The average gas-velocity curve obtained by averaging corresponding points along the cycle for six cycles is shown in figure 8(b). The deviations from this average curve are appreciable for some portions of the cycle. The streak photographs are sharp in the region plotted at a value of t/t_{cy} of 0 but generally become less distinct as this parameter approaches 1.0. Velocity measurements from the photographs for $t/t_{cy} > 0.5$ thus

contain more reading error than those taken earlier in the cycle.

The mean gas velocity or the average velocity of the combustion gases through the chamber was determined by integration of the curve of figure 8(b) over one cycle of oscillation. The mean velocity obtained by this method should agree with that calculated from the continuity equation of mass flow through the chamber:

$$V_m = \frac{\dot{w}}{\rho a} \tag{4}$$

The mean velocity determined from integration was 85 feet per second, while that calculated from equation (4) was 123 feet per second. This discrepancy can be mainly attributed to the inaccuracy of the streak-photograph measurements over the last half-cycle.

A typical pressure trace recorded on 35-millimeter film from the flush-mounted pressure transducer is reproduced in figure 9(a). This trace is a measurement of the pressure at the heat-flux probe and window location. A similar averaging technique to that used for the heat-flux output and for the streak velocities was employed to obtain the average pressure trace shown in figure 9(b). Integration of this curve indicated an average chamber pressure of 178 pounds per square inch absolute at this location.

The phase relation between chamber pressure and gas velocity measured from the

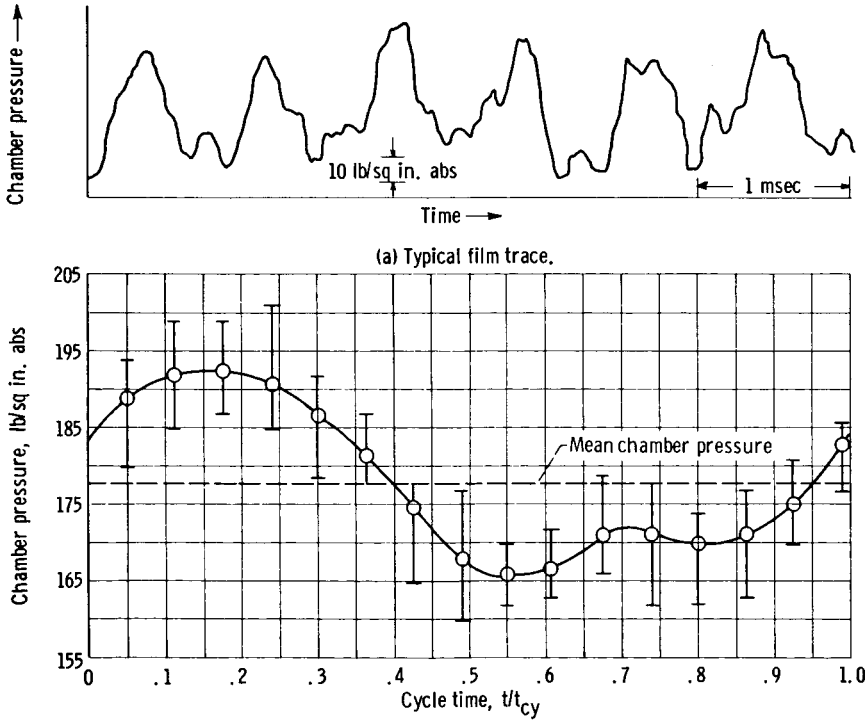

(a) Typical film trace.

(b) Chamber pressure for one cycle (averaged over seven cycles).

Figure 9. - Typical pressure transducer output and average chamber pressure for one cycle of oscillation.

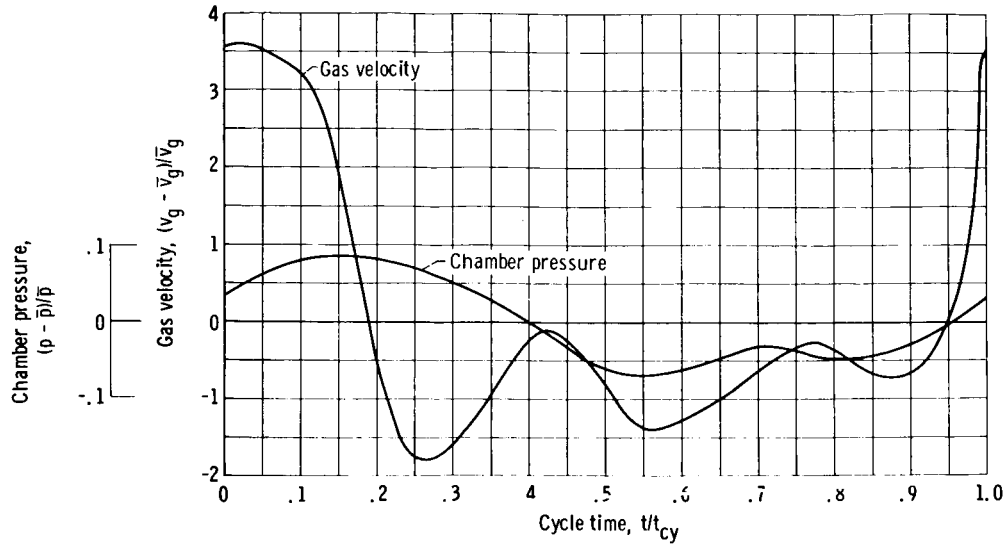

Figure 10. - Phase relation between chamber pressure and gas velocity.

streak photographs is shown in figure 10, where normalized quantities are plotted. For a cylindrical chamber possessing a pure standing acoustic longitudinal wave, the pressure leads the velocity by 90°. In figure 10, the peak pressure lags the peak velocity by about 50°. Thus, a pure standing wave does not truly exist in the chamber, but rather a distorted wave with a traveling component due to the throughput.

RESULTS AND DISCUSSION

The heat transfer to a circular cylinder depends not only on the velocity of the gases flowing past it, but also on their temperature and density. In order to obtain a velocity measurement from the output of the heat-flux probe, it was therefore necessary to determine the gas properties and their behavior. Since combustion gas temperatures were not measured directly in this study, it was necessary to approximate them. The ratio of liquid oxygen to ethanol mass flow rates in the combustor was 0.9. Gas temperature at an equilibrium composition of this oxidant-fuel ratio was calculated according to references 7 to 9. This calculated mean temperature was allowed to vary adiabatically with the pressure:

$$T_e = \bar{T}_e \left(\frac{p}{\bar{p}} \right)^{(\gamma-1)/\gamma} \tag{5}$$

where the ratio of specific heats γ was also calculated according to references 7 to 9. The value of T_e varied between 3354° and 3482° F with $\bar{T}_e = 3433^{\circ}$ F. Gas densities

were calculated from the equation of state. The maximum Reynolds number based on streak photograph velocities was 580.

Convective heat transfer for flow over cylinders is extensively reported in the literature (refs. 10 to 12). The specific equations governing this type of convective heat transfer, as reported in these references, are basically the same, although some are much more complete than others. McAdams (ref. 12) correlated heat-transfer data for laminar free-stream Reynolds numbers in the range 0.1 to 1000. His simplified relation is

$$\frac{hD_o}{k_f} = \left[0.32 + 0.47\left(\frac{\rho D_o V}{\mu_f}\right)^{0.52}\right]\left(\frac{C_p \mu_f}{k_f}\right)^{0.3} \tag{6}$$

where the thermal conductivity k_f, the dynamic viscosity μ_f, and specific heat at constant pressure C_p of the gas are evaluated at the film temperature $T_f = \frac{1}{2}(T_s + T_e)$, and the gas density ρ, at the gas temperature. The platinum surface temperature was 370° F, as determined from resistance measurements of the sensitive element and the equation

$$R_{s,h} = R_{s,c}\left[1 + \alpha(T_{s,h} - T_{s,c})\right] \tag{7}$$

where α is $0.00133/^{\circ}F$ from reference 6, and $R_{s,h}$ and $R_{s,c}$ are the hot and the cold resistance of the sensor, respectively, measured directly from the electronic circuitry. McAdams' equation (ref. 12) was used to calculate gas velocities over the sensing element in this study. Combining equations (2) and (6) yields

$$V = \left[\frac{\dfrac{C - P}{k_f \pi L (T_e - T_s)\left(\dfrac{C_p \mu_f}{k_f}\right)^{0.3}} - 0.32}{0.47\left(\dfrac{\rho D_o}{\mu_f}\right)^{0.52}}\right]^{1.923} \tag{8}$$

The resulting curve of gas velocity plotted against dimensionless time is given in figure 11 along with the velocity measured from the streak photographs. The calculated peak velocity from equation (8) was more than twice the measured value. The calculated velocity was also significantly higher than the measured velocity for the entire cycle. The region corresponding to reverse flow has been interpreted as such and is shown as a dashed line for $0.18 \leq t/t_{cy} \leq 0.35$. The two velocity curves agree well in phase. Since

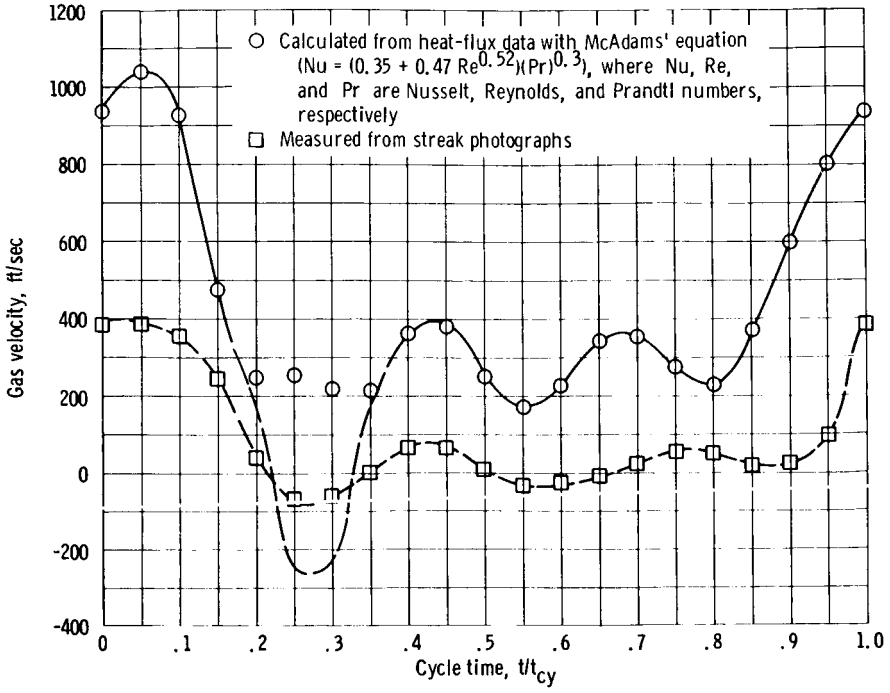

Figure 11. - Comparison of gas velocities determined from heat-flux data and from streak photographs.

the streak velocities are most nearly accurate in the region of high velocity ($t/t_{cy} \approx 0$), the velocity determination from the heat-flux measurement appears to be in error. Several possibilities exist: Other modes of heat-transfer to the sensor have not been properly accounted for; equation (8) does not apply for a high-temperature oscillating flow; or the system itself gave an erroneous reading. Each of the possibilities is discussed subsequently.

With several environmental conditions assumed for radiative heat transfer, namely, that the sensor has an absorptivity of 0.1 and is surrounded by a gas radiating as a black body at 4000° R, calculated radiation to the sensor during the combustion run was less than 1 percent of the total heat transfer. The amount of heat lost from the sensor by free convection (eq. (1)) was less than 1 percent of the heat transferred to the water for the reference condition in still air. End losses, or heat flow by conduction from the platinum through the gold or through the 96-percent-silica tube to the sensor supports, were estimated to be a maximum of 5 percent. Probe effects causing the flow velocity to be increased over the sensor were considered a possible reason for the high heat-flux signal, but the oscillatory nature of the flow prohibited a simple estimate of the probe effect. Exothermal recombination of dissociated atoms or molecules on the platinum surface should not be a problem at the low gas temperatures considered herein. None of these possible errors account for the large heat-transfer signal.

McAdams' equation was obtained by correlating the data of a number of independent

experimenters. The correlation covers steady laminar free-stream flow over a cylinder for a wide range of variables but does not include turbulent-flow data at the temperatures and pressures encountered in the combustion gas flow of this study. The validity of using McAdams' equation to describe the heat transfer to the heat-flux sensor is thus questionable. In turbulent free-stream flow, increased heat-transfer rates have been observed by a number of investigators. Some of these observations are discussed in reference 13. The effect of turbulence on heat transfer predicted in these various studies varies over a wide range. It was thus difficult to determine what correction, if any, should be made to the heat-flux data. An approximate correction for turbulence was calculated by following the procedure used in reference 13. With the assumptions that a turbulence intensity of 20 percent existed in the combustion gas flow, that the frequency of turbulence coincided with the frequency of the eddies shed by the sensing element, and that the procedure could be extrapolated to apply for lower Reynolds numbers, then an increase of 21 percent in heat transfer due to turbulence was obtained. With this increase taken into account, the calculated peak velocity was reduced to 655 feet per second. Matching of eddy frequency and free-stream turbulence frequency, however, would be coincidental. Neither the intensity nor the frequency of turbulence is well known in a combustion gas flow. Thus, it is impossible to attribute much reliability to this number because of the assumptions made.

The possibility that the sensor was not properly constructed and thus caused erroneous data was also considered. The gold film that isolated the platinum film effectively acted as a resistance in series with the platinum resistance element. If the gold layer had been deposited in a thinner layer than normal, its resistance would have been appreciable compared with that of the platinum and thus would have greatly affected the data. Resistance measurements of known lengths of gold film on a sensor were made by feeding a small current through a known resistance and the unknown resistance connected in series and separately measuring the potential drop across both resistances. The unknown resistance was then found from Ohm's Law

$$I = \frac{E_k}{R_k} = \frac{E_u}{R_u}$$

where the subscript k refers to a known resistance and the subscript u, to the unknown resistance. Although the measurement proved to be somewhat inaccurate in that three results for different samples of the gold film differed by a factor of more than two, the measurements did show that the gold resistance was an appreciable fraction (approximately one-eighth) of the total sensor resistance. This fact meant that all the heat generated electrically was not dissipated in the platinum film but that a significant heat loss also occurred in the gold film.

Thus, either free-stream turbulence or sensor construction may have affected the heat-flux sensor output. It was impossible to determine the magnitude of the effect for either source of error. In figure 12, a constant power level of 23 Btu per hour is subtracted from the heat-flux signal and the velocity recalculated by use of equation (8). By applying a constant correction to the signal, it was thus possible to obtain velocities which agreed well with the measured velocities from the streak photographs. Obviously, a method such as this one is not satisfactory for absolute velocity measurements.

Ordinarily, velocity measuring devices are calibrated in known velocity and temperature flow streams before being used in test streams. Because physical changes take place so easily in the sensor and because of the difficulty in simulating a combustion gas environment in which the temperature, density, and velocity are known, no calibration of the heat-flux sensor was attempted in this study. The similarity of the phasing of the two curves in figure 12, however, shows that velocity was actually being sensed.

As an independent check on velocity, the average pressure trace of figure 9(b) (p. 11) and the equation of motion of sound waves in a gas were used to calculate gas velocities in the rocket combustor. An equation in terms of sines and cosines was fitted to the average chamber pressure trace and resulted in

$$p = \bar{p} + \sum_{n=1}^{5} (K_n \cos n\varphi + K_n' \sin n\varphi) \tag{9}$$

When equation (9) was rewritten in terms of chamber position and the equation of motion for an acoustic wave from reference 14,

$$\frac{\partial u}{\partial t} = -\frac{1}{\rho}\frac{\partial p}{\partial x} \tag{10}$$

was used, the fluctuating component of the gas particle velocity expression became

$$u = -\frac{c}{\gamma \bar{p}} \sum_{n=1}^{5} (M_n \cos n\varphi + M_n' \sin n\varphi) \tag{11}$$

This velocity fluctuated about the mean velocity calculated in equation (4). The resulting velocity trace is shown in figure 13 and is compared with the velocity from the streak photographs. The maximum velocity found by either technique agrees to within 3 percent, which indicates that the simplified technique can be used to obtain the maximum combustor velocity.

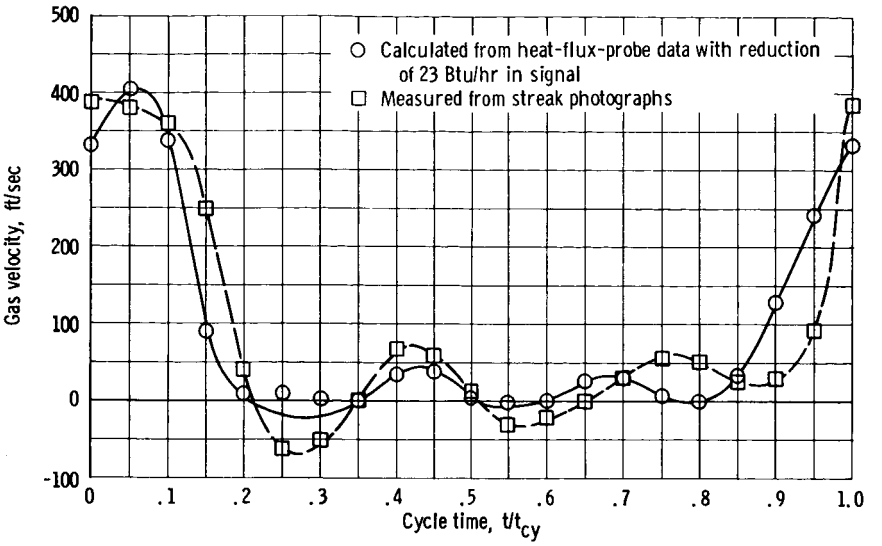

Figure 12. - Comparison of gas velocities calculated with reduced signal by use of equation (8) with velocities measured from streak photographs.

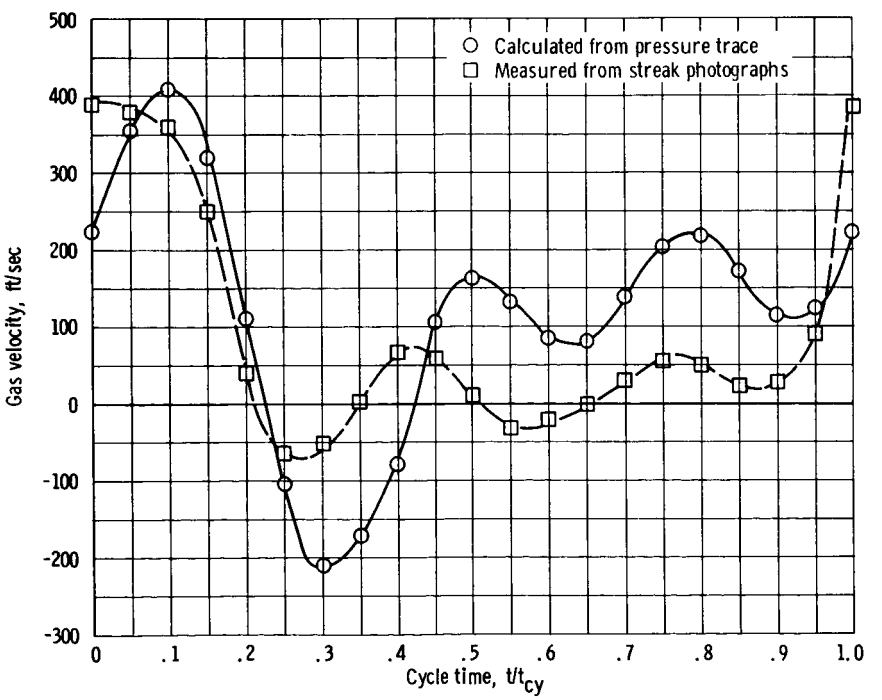

Figure 13. - Comparison of gas velocities determined from pressure trace and streak photographs.

Gas velocity measurements in a rocket combustor can thus be obtained by three different techniques, each with its advantages and shortcomings.

Velocity calculations made from the heat-flux-sensor signal gave velocities considerably higher than those measured with streak photographs or calculated from pressure measurements. If the heat-flux signal was reduced by a constant value, the calculated velocities agreed qualitatively with the measured streak velocities in the region where the streak photographs are most reliable (i.e., $0 \leq t/t_{cy} \leq 0.5$). Lack of physical strength, nonuniformities between sensors, and even nonuniformities within an individual sensor place limitations on the sensor as a tool for oscillating combustion environment applications. Absolute gas velocity measurements are difficult to obtain when the system is used in studies such as this. Useful relative velocity behavior can be obtained if the sensors are rugged enough to withstand the environment. The heat-flux system can work successfully and give absolute velocity measurements in homogeneous, lower velocity, lower temperature gas streams. The sensor allows nearly instantaneous point measurements.

The streak photographs obtained herein provide the most accurate method of determining the maximum velocity in the combustor. By their very nature, streak photographs provide the most easily read and accurate velocities in regions where there are large gradients in temperature and concentration of the radiating gases. Streak photographs of velocities near zero or in a homogeneous gas are not sharp, and accurate measurements cannot be made.

The simplest method of obtaining the maximum gas velocity in a combustion chamber appears to be with a single pressure measurement. The calculated maximum particle velocity agrees to within 3 percent with the maximum measured streak velocity.

SUMMARY OF RESULTS

Combustion gas velocities in an unstable rocket combustor were measured by three techniques. The results are summarized as follows:

1. The output of a water-cooled, thin-film, heat-flux probe was used to determine local instantaneous gas velocity behavior qualitatively in a high-temperature, oscillatory combustion gas stream, but its use was limited for absolute velocity measurements in such flows.

2. Maximum velocity measured from streak photographs and maximum velocity calculated from static-pressure measurements agreed to within 3 percent. Streak photo-

graphs were most easily obtained if gradients in temperature and concentration of radiating gases were high. Static-pressure measurements presented the simplest method of obtaining maximum velocity.

Lewis Research Center,
National Aeronautics and Space Administration,
Cleveland, Ohio, September 28, 1966,
128-31-06-02-22.

APPENDIX - SYMBOLS

A	surface area of sensor, sq ft
a	cross-sectional area of chamber, sq ft
C	constant heat-transfer rate from sensor to cooling water, Btu/hr
C_p	specific heat at constant pressure, Btu/(lb mass)(^oF)
c	speed of sound
D_o	sensor diameter, ft
E_k	voltage drop across known resistance, V
E_u	voltage drop across gold film, V
h	heat-transfer coefficient between environment and sensor surface, Btu/(hr)(ft^2)(^oF)
I	current supplied to sensor, A
K_n, K_n'	constants
k_f	thermal conductivity of gas evaluated at film temperature, Btu/(hr)(ft)(^oF)
L	sensor length, ft
ℓ	combustion length, ft
M_n	$K_n' \tan (n\pi x/\ell)$
M_n'	$-K_n \tan (n\pi x/\ell)$
m	magnification
n	integer, 1, 2, . . ., 5
P	power supplied to sensor, Btu/hr
p	absolute chamber pressure, lb force/sq in.
$\bar{p}$	average absolute chamber pressure, lb force/sq in.
Q	heat-transfer rate from combustion environment to sensor, Btu/hr
R_k	known resistance, ohms
R_s	sensor resistance, ohms
$R_{s,c}$	sensor resistance cold, ohms
$R_{s,h}$	sensor resistance hot, ohms
R_u	resistance of gold films, ohms
R_1	variable resistance in Wheatstone bridge, ohms
R_2, R_3	fixed resistances in Wheatstone bridge, ohms
T_e	instantaneous environment temperature, ^oF
$\bar{T}_e$	average environment temperature, ^oF
T_f	film temperature, $(T_s + T_e)/2$, ^oF
T_s	sensor surface temperature, ^oF
$T_{s,c}$	sensor temperature cold, ^oF
$T_{s,h}$	sensor temperature hot, ^oF
T_w	cooling water temperature, ^oF
t	time, msec
t_{cy}	time for one cycle of oscillation, msec

U	heat-transfer coefficient between sensor surface and cooling water based on sensor surface area, Btu/(hr)(ft^2)($^\circ$F)
u	fluctuating gas velocity, ft/sec
V	gas velocity calculated from heat-flux data, ft/sec
V_m	mean gas velocity calculated from continuity equation, ft/sec
v_f	film speed, ft/sec
v_g	gas velocity measured from streak photographs, ft/sec
$\overline{v}_g$	average gas velocity measured from streak photographs, ft/sec
$\dot{w}$	mass flow rate, lb mass/sec
x	distance measured from injector along combustor axis, ft
α	temperature coefficient of resistance, 1/$^\circ$F
γ	ratio of specific heats
θ	angle between vertical axis and streak, rad
μ_f	dynamic viscosity of gas evaluated at film temperature, lb mass/(ft)(hr)
ρ	gas density, lb mass/cu ft
φ	angle along cycle, rad

REFERENCES

1. Wieber, Paul R.; and Mickelsen, William R.: Effect of Transverse Acoustic Oscillations on the Vaporization of a Liquid-Fuel Droplet. NASA TN D-287, 1960.

2. Ingebo, Robert D.: Atomization of Ethanol Jets in a Combustor with Oscillatory Combustion-Gas Flow. NASA TN D-3513, 1966.

3. Heidmann, M. F.; and Auble, C. M.: Injection Principles from Combustion Studies in a 200-Pound-Thrust Rocket Engine Using Liquid Oxygen and Heptane. NACA RM E55C22, 1955.

4. Blackshear, P. L.; and Fingerson, L. M.: Some New Measuring Techniques in High Temperature Gases. Tech. Rep. No. 61-3, Combustion Lab., Univ. of Minnesota, Sept. 1961.

5. Fingerson, Leroy M.; and Blackshear, Perry L., Jr.: Heat Flux Probe for Dynamic Measurements in High-Temperature Gases. Temperature- Its Measurement and Control in Science and Industry, vol. 3, pt. 2, A. I. Dahl, ed., Reinhold Publ. Corp., 1962, pp. 655-663.

6. Fingerson, L. M.: Research on the Development and Evaluation of a Two-Sensor Enthalpy Probe. (AFARL-64-161, DDC No. AD-608605), Thermo-Systems, Inc., Oct. 1964.

7. McBride, Bonnie J.; Heimel, Sheldon; Ehlers, Janet G.; and Gordon, Sanford: Thermodynamic Properties to 6000° K for 210 Substances Involving the First 18 Elements. NASA SP-3001, 1963.

8. Gordon, Sanford; and Zeleznik, Frank J.: A General IBM 704 or 7090 Computer Program for Computation of Chemical Equilibrium Compositions, Rocket Performance, and Chapman-Jouquet Detonations. Supplement I - Assigned Area-Ratio Performance. NASA TN D-1737, 1963.

9. Zeleznik, Frank J.; and Gordon, Sanford: A General IBM 704 or 7090 Computer Program for Computation of Chemical Equilibrium Compositions, Rocket Performance, and Chapman-Jouquet Detonations. NASA TN D-1454, 1962.

10. Collis, D. C.; and Williams, M. J.: Two-Dimensional Convection from Heated Wires at Low Reynolds Number. J. Fluid Mech., vol. 6, pt. 3, Oct. 1959, pp. 357-384.

11. King, Louis V.: On the Convection of Heat from Small Cylinders in a Stream of Fluid: Determination of the Convection Constants of Small Platinum Wires with Applications to Hot-Wire Anemometry. Roy. Soc. Phil. Trans., Ser. A, vol. 214, 1914, pp. 373-432.

12. McAdams, William H.: Heat Transmission. 3rd ed., McGraw Hill Book Co., Inc., 1954.

13. Hegge Zijnen, B. G. van der: Heat Transfer from Horizontal Cylinders to a Turbulent Air Flow. Appl. Sci. Res., Sec. A, vol. 7, 1958, pp. 205-223.

14. Morse, Philip M.: Vibration and Sound. 2nd ed., McGraw Hill Book Co., Inc., 1948.

"The aeronautical and space activities of the United States shall be conducted so as to contribute . . . to the expansion of human knowledge of phenomena in the atmosphere and space. The Administration shall provide for the widest practicable and appropriate dissemination of information concerning its activities and the results thereof."

—NATIONAL AERONAUTICS AND SPACE ACT OF 1958

NASA SCIENTIFIC AND TECHNICAL PUBLICATIONS

TECHNICAL REPORTS: Scientific and technical information considered important, complete, and a lasting contribution to existing knowledge.

TECHNICAL NOTES: Information less broad in scope but nevertheless of importance as a contribution to existing knowledge.

TECHNICAL MEMORANDUMS: Information receiving limited distribution because of preliminary data, security classification, or other reasons.

CONTRACTOR REPORTS: Technical information generated in connection with a NASA contract or grant and released under NASA auspices.

TECHNICAL TRANSLATIONS: Information published in a foreign language considered to merit NASA distribution in English.

TECHNICAL REPRINTS: Information derived from NASA activities and initially published in the form of journal articles.

SPECIAL PUBLICATIONS: Information derived from or of value to NASA activities but not necessarily reporting the results of individual NASA-programmed scientific efforts. Publications include conference proceedings, monographs, data compilations, handbooks, sourcebooks, and special bibliographies.

Details on the availability of these publications may be obtained from:

SCIENTIFIC AND TECHNICAL INFORMATION DIVISION

NATIONAL AERONAUTICS AND SPACE ADMINISTRATION

Washington, D.C. 20546